RSC Advances

PAPER

View Article Online
View Journal | View Issue

Check for updates

Cite this: *RSC Adv.*, 2025, **15**, 5795

Vinasse photoreforming for hydrogen production using Pt/TiO_2 as catalyst under UV irradiation

Patrícia Ferreira Silvaino, João Coutinho Ferreira, Saulo Amaral Carminati, * Jorge Moreira Vaz and Estevam Vitorio Spinacé *

Received 20th January 2025
Accepted 15th February 2025

DOI: 10.1039/d5ra00481k

rsc.li/rsc-advances

Vinasse, a dark-colored aqueous byproduct of bioethanol production, contains a variety of organic compounds and inorganic salt ions. In this study, the photoreforming of vinasse was investigated using Pt/TiO_2 as a catalyst under UV irradiation. The gaseous products generated were analyzed, revealing the formation of hydrogen (H_2) along with other gases, including CO_2, CH_4, CO, C_2H_6, C_2H_4, C_3H_8, and C_4H_{10}. When using filtered vinasse, H_2 and other gaseous products were produced solely through photolysis, even in the presence of the Pt/TiO_2 photocatalyst. Notably, photocatalytic H_2 production was observed when inorganic salt ions were removed from the vinasse, and a lower concentration of vinasse was employed in the reaction medium.

Open Access Article. Published on 20 February 2025. Downloaded on 2/20/2026 6:57:31 AM.
This article is licensed under a Creative Commons Attribution-NonCommercial 3.0 Unported Licence.

1. Introduction

The environmental impacts have stimulated the use of renewable sources in the chemical industry, however, more than 90% of hydrogen (H_2) continues to be produced by reforming fossil fuel feedstocks.[1]

The photocatalytic H_2 production over nanostructured semiconductors has the advantage of renewable energy utilization and a common strategy involves the use of substrates such as methanol, ethanol and others to overcome the large thermodynamic barrier of the oxygen evolution reaction and the recombination of photogenerated charge carriers.[2] On the other hand, the high cost of these substrates is an obstacle to achieving practical applications. In this sense, the low cost and easy accessibility of agricultural biomass and waste have attracted significant interest as potential substrates.[3]

Brazil is the second largest producer of bioethanol, which is primarily through sugarcane fermentation, generating vinasse as the main byproduct. Vinasse is an aqueous dark-colored waste containing organic compounds (residual sugars, glycerol, mannitol, organic acids and phenolic compounds) and inorganic salt ions (sodium, potassium, calcium, and magnesium cations, and chloride, nitrate, nitrite, phosphate, and sulfate anions). Due to the large volumes of vinasse resulting from bioethanol production, at least 10–15 liters for every 1 liter of ethanol, its disposal and/or use has become a major challenge. In Brazil, during the 1980s, fertigation became a widespread practice, leading to soil salinization and the leaching of metals into groundwater.[4,5]

More recently, other processes, such as anaerobic digestion of vinasse to produce biogas are being evaluated and developed.[6,7] Additionally, the vinasse photocatalytic degradation for decolorization and total organic carbon removal is another process that has been extensively investigated.[8,9]

The photocatalytic water splitting over nanostructured semiconductors for H_2 production offers the advantage of renewable energy utilization. A common strategy involves the use of sacrificial agents (SAs) such as methanol, ethanol and others to overcome the large thermodynamic barrier of oxygen the evolution reaction and mitigate the recombination of photogenerated charge carriers.[2] On the other hand, the high cost of SAs presents a significant obstacle to achieve practical applications, making low-cost and easily accessible SAs, such as biomass and organic wastes, increasingly attractive.[10]

While biomass-derived substrates like glucose, polysaccharides, glycerol, lignin and cellulose have been investigated as SAs for photocatalytic H_2 production,[11–16] the use of raw waste materials has been less explored.[17] Additionally, the photoreforming of vinasse over semiconductor-based photocatalysts for H_2 production has not yet been explored.[8]

TiO_2 has been considered one of the most promising light-harvesting materials for H_2 production from water due to its low cost and stability. However, it is only activated by UV light, which corresponds to about 5% of the sunlight spectrum. Furthermore, the main limitation of sunlight-driven photoreactors is their low efficiency on cloudy days and at night. An alternative would be to use artificial light, such as a UV-LED photoreactor powered by renewable energy, to overcome these challenges and improve the efficiency of TiO_2 photocatalysts.[18]

In this work, we explore the photoreforming of vinasse for H_2 production using Pt/TiO_2, the most common reference photocatalyst using UV irradiation.[19] This approach could not only

Instituto de Pesquisas Energéticas e Nucleares, IPEN/CNEN, Av. Prof. Lineu Prestes, 2242-Cidade Universitária, São Paulo, SP, 05508-000, Brazil. E-mail: saulocarminati89@gmail.com; espinace@ipen.br

© 2025 The Author(s). Published by the Royal Society of Chemistry

Open Access Article. Published on 20 February 2025. Downloaded on 2/20/2026 6:57:31 AM.
This article is licensed under a Creative Commons Attribution-NonCommercial 3.0 Unported Licence.

mitigate waste by improving resource efficiency but also contribute to more sustainable energy systems.

2. Experimental

2.1. Materials and methods

2.1.1. Materials. The following reagents and solvents were used: TiO_2 P25 (Evonik), $H_2PtCl_6 \cdot 6H_2O$ (Sigma-Aldrich®), Ethylene glycol (Dinâmica Química), ultrapure deionized water (18.2 MΩ cm, 25 °C) and ethyl alcohol (Sigma-Aldrich®, 99.5% purity).

2.1.2. Vinasse treatment. Raw vinasse from Usina Colombo, Ariranha, São Paulo State, Brazil, was filtered (vinasse F) on a paper filter to separate the liquid phase from the solid phase. In a further step, the inorganic metal salts (cations and anions) of the vinasse F were removed by ion-exchange (IE) process passing through a column of cation exchange resin (Amberlite IRC-748) and a column of anion exchange resin (Dowex-3) to remove the ionic species.

2.1.3. Synthesis and characterization of Pt/TiO_2 photocatalyst. The Pt/TiO_2 photocatalyst was prepared with 0.5 wt% of Pt content by an alcohol-reduction method.[20,21] $H_2PtCl_6 \cdot 6H_2O$ was dissolved in an ethylene glycol : water solution (3 : 1 v/v) and the TiO_2 P25 was dispersed in this solution. The resulting mixture was stirred and heated under reflux at 180 °C for 2 h. Afterwards, the mixture was centrifuged (9000 rpm), and a light gray solid was obtained. The solid was washed with excess deionized water and dried at 90 °C for 24 h.

The elemental composition of the Pt/TiO_2 was determined by WD-XRF (Wavelength-Dispersive X-ray Fluorescence) in a Rigaku Supermini200 spectrometer (Pd source, 50 kV, 200 W, zirconium filter) using a calibration curve. The shape, size and dispersion of the Pt nanoparticles on the TiO_2 support were analyzed by TEM (Transmission Electron Microscopy) using a JEOL microscope, model JEM-2100 (200 kV). Photoluminescence (PL) spectra were performed in an Ocean Optics 2000 luminescence spectrometer + USB spectrometer with a CCD camera, from 200 to 1000 nm. The excitation wavelength was 265 nm, and the spectra were recorded at room temperature in the range of 200–1000 nm, with the scanning speed at 1000 nm min^{-1}, and the PMT voltage was 650 V. Raman spectroscopy measurements were obtained with a Horiba Scientific Macro-Ram Raman spectrometer using a 785 nm wavelength laser. UV-Vis spectra of the vinasse solution before and after UV irradiation were recorded by using a Varian UV-Vis spectrometer model Cary 50 from 200 to 800 nm.

2.1.4. Photocatalytic activity. The photoreforming experiments were performed in a system using a commercial Ace 250 mL photoreactor coupled with a gas chromatograph (GC) Agilent 7890B-mass spectrometer MSD 5977B system. The GC has a thermal conductivity detector (TCD), a methanizer and a flame ionization detector (FID). Two columns were used in order to separate the reaction products, a plot U and molecular sieve 5 Å column. Calibration curves were made using two certified gas mixtures to quantify CO_2, C_2H_4, C_2H_6, C_3H_8, C_4H_{10}, H_2, CH_4 and CO. The detection limits were 0.001% for CO_2 and C_2–C_4; 0.008% for CH_4 and CO and 0.3% for H_2. In a typical experiment, 75 mg of the Pt/TiO_2 photocatalyst was dispersed in 250 mL of vinasse/water solution (v/v) and a continuous flow of He gas (25 mL min^{-1}) was bubbled into this suspension for 16 h before the beginning of the experiment to purge the O_2. During the experiments, He (25 mL min^{-1}) was used as carrier gas and a 450 W Hg lamp (UV A/B/C) as a light source. Two cooling systems were used, one for cooling the Hg lamp operating at 40 °C and one coupled to a condenser at the output of the reactor connected to the CG system to condense the water (15 °C). In this manner, the photoreforming reactions were performed at a temperature close to 50 °C.

3. Results and discussion

For Pt/TiO_2 photocatalyst, the Pt amount determined by WDXRF was 0.52 wt%, which is very close to the nominal value. Fig. 1 shows the TEM micrograph and histogram of the Pt/TiO_2 photocatalyst, where the Pt nanoparticles (small black dots) are clearly visible, exhibiting good dispersion on the TiO_2 support, with sizes ranging from 2 to 5 nm.

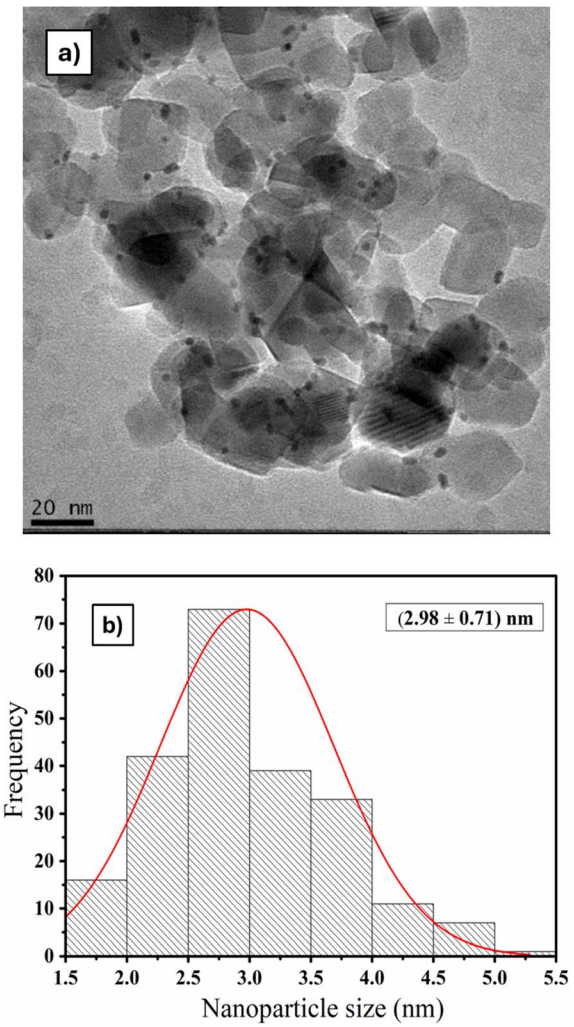

Fig. 1 (a) TEM micrograph and (b) histogram of Pt/TiO_2 photocatalyst.

© 2025 The Author(s). Published by the Royal Society of Chemistry

Open Access Article. Published on 20 February 2025. Downloaded on 2/20/2026 6:57:31 AM.
This article is licensed under a Creative Commons Attribution-NonCommercial 3.0 Unported Licence.

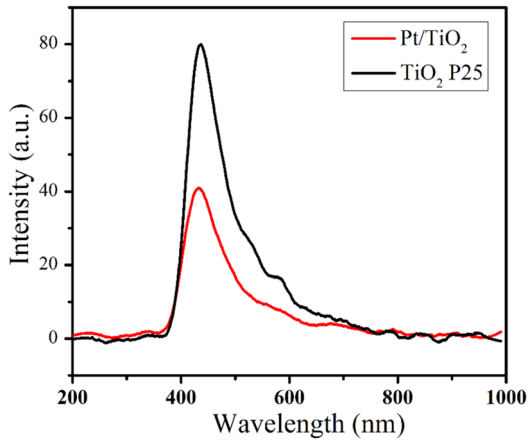

Fig. 2 PL spectra of TiO_2 P25 commercial and Pt/TiO_2 photocatalyst.

The PL spectra of the Pt/TiO_2 photocatalyst and TiO_2 P25 support are shown in Fig. 2, and they exhibit similar profiles, with emission peaks centered at 431 and 436 nm for Pt/TiO_2 and TiO_2 P25, respectively. The emission peak of the Pt/TiO_2 photocatalyst has lower intensity compared to the peak of the TiO_2 P25 support, indicating a decrease in the recombination rate of the electron–hole pairs.[22,23]

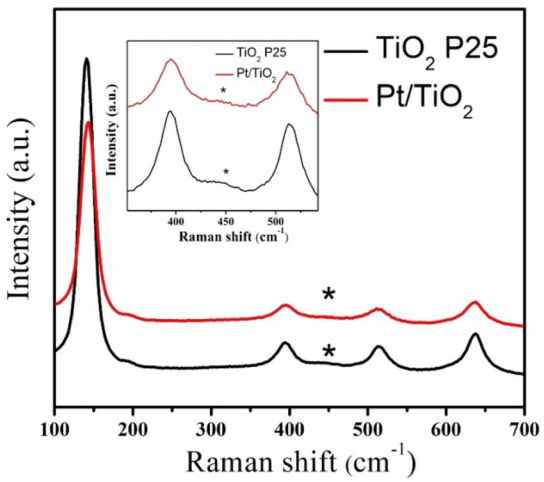

Fig. 3 Raman spectra of commercial TiO_2 P25 and Pt/TiO_2 photocatalyst.

The Raman spectra of the Pt/TiO_2 photocatalyst and TiO_2 P25 support are shown in Fig. 3. The spectrum of TiO_2 P25 presented peaks centered at 140, 196, 394, 514 and 636 cm^{-1}, which are attributed to the vibrational modes of the anatase phase, with a small peak at 445 cm^{-1} corresponding to the rutile phase. These peaks are characteristic of TiO_2 P25 support, which contains a mixture of both anatase and rutile phases.[24,25] The Pt/TiO_2 photocatalyst presented a similar profile, but with a small positive shift of 3 cm^{-1} in the most intense peak, which is associated with the interactions between Pt nanoparticles the TiO_2 support.[26,27]

The photoreforming experiments are shown in Table 1. Initially, vinasse F (with the liquid phase separated from the solid phase by filtration) was tested using a vinasse F : H_2O ratio of 50/50 (v/v) under UV irradiation. The products identified in the gas phase followed this order of formation rates: CO_2 > H_2 > CO > C_2H_6 > CH_4 > C_3H_8 > C_4H_{10} > C_2H_4. These products were formed through photochemical reactions (photolysis) since no Pt/TiO_2 photocatalyst was added to the reaction medium. On the other hand, the addition of Pt/TiO_2, the most common reference photocatalyst under UV irradiation,[28] practically did not alter the products formed or their formation rates. Even when the amount of Pt/TiO_2 was doubled (150 mg), the results remained unchanged. UV-Vis absorption spectra of vinasse (F) solution (50/50), after UV irradiation, and after UV irradiation in the presence of Pt/TiO_2 as photocatalyst, are shown in Fig. 4.

The UV-Vis spectrum of vinasse (F) showed absorption bands in the UV region (200–400 nm) and their intensities were reduced after the photoreaction under UV irradiation indicating the degradation of vinasse by photolysis. However, when the photoreaction was carried out in the presence of Pt/TiO_2 as photocatalyst, the intensities and the shape of the absorption bands were very similar to those observed for the reaction conducted only with UV light, showing that photochemical reactions (photolysis) predominated even in the presence of the photocatalyst. Therefore, under these conditions, the H_2 production primarily results from the photolysis of vinasse rather than from photocatalytic process. It is likely that some organic or inorganic compounds in vinasse inhibit UV light absorption by the photocatalyst and/or block the surface catalytic sites.[29]

Vinasse contains appreciable amounts of inorganic salt ions,[5] and some of these ionic species could absorb UV light in

Table 1 Products formation rates in the gas phase of vinasse photoreforming (75 mg of photocatalyst, 250 mL vinasse + H_2O, 25 mL min^{-1} He, 450 W Hg lamp)[a]

		Products formation rates (μmol g_{cat}^{-1} h^{-1})							
Vinasse/photocatalyst	Vinasse/H_2O (v/v)	C_2H_6	C_2H_4	C_3H_8	C_4H_{10}	CH_4	CO	CO_2	H_2
Vinasse F/without	50/50	407	12	123	21	157	909	4148	2004
Vinasse F/(Pt/TiO_2)	50/50	512	23	163	24	178	994	5248	2200
Vinasse IE/without	50/50	2113	159	552	257	1792	973	13 254	2827
Vinasse IE/(Pt/TiO_2)	50/50	2089	224	591	280	1665	1096	15 759	4619
Vinasse IE/without	10/90	572	9	166	56	1068	527	4449	1787
Vinasse IE/(Pt/TiO_2)	10/90	422	20	147	46	963	530	5685	5252

[a] For comparative purposes.

Open Access Article. Published on 20 February 2025. Downloaded on 2/20/2026 6:57:31 AM.
This article is licensed under a Creative Commons Attribution-NonCommercial 3.0 Unported Licence.

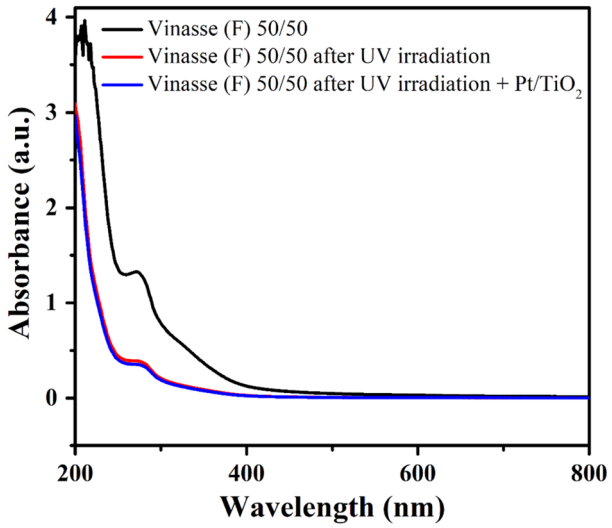

Fig. 4 UV-Vis absorption spectra of vinasse (F) SA/H_2O of 50/50, after UV irradiation and after UV irradiation in the presence of Pt/TiO_2.

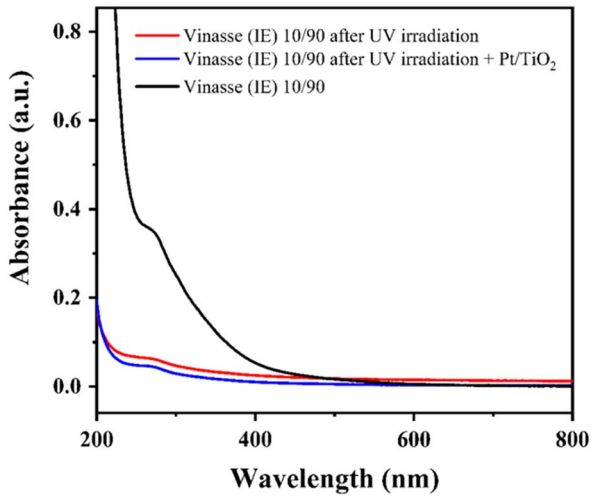

Fig. 5 UV-Vis absorption spectra of vinasse (IE) 10/90 before and after UV irradiation, and after UV irradiation in the presence of Pt/TiO_2.

aqueous solution,[30] as well as potentially lead to the deactivation of the photocatalysts.[31,32]

To eliminate the influence of these species, vinasse F was treated by an ion-exchange process (IE) and tested using vinasse : H_2O ratio of 50/50 under UV irradiation. As a result, an increase in the formation rates of all products was observed compared to vinasse F. Interestingly, when this photoreaction took place in the presence of Pt/TiO_2 photocatalyst and under UV irradiation, an increase in CO_2 and H_2 (4619 μmol g_{cat}^{-1} h^{-1}) formation rates was observed, while the formation of other products remained practically unchanged. Thus, two simultaneous processes may be occurring, a photochemical and a photocatalytic process, both of which contribute to the increased CO_2 and H_2 production.

Recently, Wongyongnoi *et al.*[17] described the green synthesis of H_2 and the decolorization of distillery effluent using Au/TiO_2 as photocatalyst. However, neither H_2 production nor decolorization was achieved using fresh distillery effluent, even in the presence of the photocatalyst and UV irradiation. Under the studied conditions, the maximum H_2 production (52.5 μmol g_{cat}^{-1} h^{-1}) with 64.4% decolorization was achieved only with 100-fold diluted distillery effluent and the addition of 15 vol% of ethanol, which also served as a sacrificial agent, to the reaction medium. In a similar study, Iervolino *et al.*[33] described the simultaneous valorization and treatment of olive mill wastewater (OMW) through a photocatalytic process to produce hydrogen and reduce the polluting load of this waste, using a home-made sol–gel TiO_2 as photocatalyst. The best results were obtained using a dilution of OMW at 1 : 70 with deionized water, yielding a H_2 production of about 4200 μmol g_{cat}^{-1} h^{-1}.

In this way, the volume of vinasse IE (vinasse : H_2O ratio of 10 : 90) was reduced in the reaction medium (Table 1). Under UV irradiation, a decrease in the formation rates of all products was observed compared to the vinasse : H_2O ratio of 50 : 50. On the other hand, when the photoreaction was performed in the presence of Pt/TiO_2 photocatalyst, a more pronounced increase in the CO_2 and H_2 formation was observed.

UV-Vis spectra of vinasse (IE) (10/90) after UV irradiation and after UV irradiation in the presence of Pt/TiO_2 as photocatalyst are shown in Fig. 5. The intensities of the absorption bands of the photoreaction performed in the presence of Pt/TiO_2 photocatalyst were reduced compared to the reaction performed only under UV irradiation, indicating more effective vinasse degradation. Under these conditions, the use of a lower concentration of vinasse appears to facilitate UV light absorption by the photocatalyst, making the H_2 production through the photocatalytic process more effective. Despite this, there is also a significant increase in CO_2 production. Therefore, the enhanced production of H_2 and CO_2 observed in the presence of the Pt/TiO_2 photocatalyst may be associated with the activation of H_2O molecules by holes ($H_2O + h^+ \rightarrow \cdot OH + H^+$), leading to the formation of highly reactive and non-selective ·OH radical, which favor the complete oxidation of vinasse to CO_2. Meanwhile, the photogenerated electrons are attracted to the Pt sites, where the reduction of H^+ to H_2 occurs.[34,35]

4. Conclusion

The photoreforming of the liquid phase of raw vinasse (vinasse F/H_2O ratio of 50/50) under UV irradiation resulted in the production of H_2, CO_2, CO, and C_2–C_4 hydrocarbons through a photochemical process. On the other hand, the addition of Pt/TiO_2 photocatalyst did not alter the products or their formation rates, suggesting that no photocatalytic activity occurred under these conditions. In contrast, using ion-exchanged vinasse (vinasse IE) under UV irradiation in conjunction with the Pt/TiO_2 photocatalyst led to an increase in H_2 and CO_2 production, indicating that photocatalytic processes were indeed occurring. However, the photochemical process still remained dominant. Under the studied conditions, the photocatalytic H_2 production was enhanced using vinasse IE and by reducing its

© 2025 The Author(s). Published by the Royal Society of Chemistry

Open Access Article. Published on 20 February 2025. Downloaded on 2/20/2026 6:57:31 AM. This article is licensed under a Creative Commons Attribution-NonCommercial 3.0 Unported Licence.

concentration in the reaction medium (vinasse IE/H_2O volume ratio of 10/90). Therefore, further investigation into the photoreforming of vinasse is warranted, and ongoing studies aim to optimize process conditions and identify more effective photocatalysts.

Data availability

The data that support the findings of this study are available from the authors.

Author contributions

Patricia F. Silvaino: photocatalysts preparation and characterization, photochemical experiments, data curation, editing, review. João C. Ferreira: vinasse treatments, editing, review. Saulo A. Carminati: data curation, writing-original draft, editing, review, proofreading manuscript; Jorge M. Vaz: conceptualization, investigation, data curation, supervision, editing, review; Estevam V. Spinacé: conceptualization, investigation, data curation, supervision, writing-original draft, editing, review, proofreading. All authors commented on previous versions of the manuscript. All authors read and approved the final manuscript.

Conflicts of interest

The authors declare that no competing financial interests or personal relationships influenced the work reported in this paper.

Acknowledgements

The authors gratefully acknowledge support from São Paulo Research Foundation (FAPESP – Grant number 2021/01896-4) and from Brazilian National Council for Scientific Development (CNPq – Grant number 407967/2022-2 and 384264/2023-9). We also thank the support given by Arthur P. Machado from "Laboratório de Nanotecnologia e Energia Solar", Chemistry Institute, UNICAMP for providing the facilities of photoluminescence experiments.

References

1 B. Parkinson, P. Balcombe, J. F. Speirs, A. D. Hawkes and K. Hellgardt, *Energy Environ. Sci.*, 2019, **12**, 19–40.
2 C. Shi, F. Kang, Y. Zhu, M. Teng, J. Shi, H. Qi, Z. Huang, C. Si, F. Jiang and J. Hu, *Chem. Eng. J.*, 2023, **452**, 138980.
3 T. Zhang and S. Lu, *Chem Catal.*, 2022, **2**, 1502–1505.
4 G. C. Rego, T. B. Ferreira, L. R. Ramos, C. A. de Menezes, L. A. Soares, I. K. Sakamoto, M. B. A. Varesche and E. L. Silva, *Biomass Convers. Biorefin.*, 2022, **12**, 5527–5541.
5 M. S. Silverio, R. P. Calegari, G. M. F. L. Leite, L. M. L. M. Prado, B. C. Martins, E. A. da Silva, J. P. Neto, A. Gomig and A. S. Baptista, *Braz. J. Biol. Sci.*, 2021, **15**, 42–68.
6 A. Montiel-Rosales, N. Montalvo-Romero, L. E. García-Santamaría, L. C. Sandoval-Herazo, H. Bautista-Santos and G. Fernández-Lambert, *Sustainability*, 2022, **14**, 11635.
7 J. C. de Carvalho, L. P. de Souza Vandenberghe, E. B. Sydney, S. G. Karp, A. I. Magalhães, W. J. Martinez-Burgos, A. B. P. Medeiros, V. Thomaz-Soccol, S. Vieira, L. A. J. Letti, C. Rodrigues, A. L. Woiciechowski and C. R. Soccol, *Fermentation*, 2023, **9**, 349.
8 L. L. Nascimento, R. A. Carvalho Souza, J. Zacour Marinho, C. Wang and A. O. T. Patrocinio, *J. Cleaner Prod.*, 2024, **449**, 141709.
9 A. Montiel-Rosales, N. Montalvo-Romero, L. E. García-Santamaría, L. C. Sandoval-Herazo, H. Bautista-Santos and G. Fernández-Lambert, *Sustainability*, 2022, **14**, 11635.
10 T. Zhang and S. Lu, *Chem Catal.*, 2022, **2**, 1502–1505.
11 A. Speltini, M. Sturini, D. Dondi, E. Annovazzi, F. Maraschi, V. Caratto, A. Profumo and A. Buttafava, *Photochem. Photobiol. Sci.*, 2014, **13**, 1410–1419.
12 K. A. Davis, S. Yoo, E. W. Shuler, B. D. Sherman, S. Lee and G. Leem, *Nano Convergence*, 2021, **8**, 6.
13 G. Zhang, C. Ni, X. Huang, A. Welgamage, L. A. Lawton, P. K. J. Robertson and J. T. S. Irvine, *Chem. Commun.*, 2016, **52**, 1673–1676.
14 H. Zhao, J. Liu, N. Zhong, S. Larter, Y. Li, M. G. Kibria, B.-L. Su, Z. Chen and J. Hu, *Adv. Energy Mater.*, 2023, **13**, 2300257.
15 J. Ma, K. Liu, X. Yang, D. Jin, Y. Li, G. Jiao, J. Zhou and R. Sun, *ChemSusChem*, 2021, **14**, 4903–4922.
16 X. Xu, L. Shi, S. Zhang, Z. Ao, J. Zhang, S. Wang and H. Sun, *Chem. Eng. J.*, 2023, **469**, 143972.
17 P. Wongyongnoi, K. Serivalsatit, M. Hunsom and K. Pruksathorn, *Int. J. Hydrogen Energy*, 2024, **80**, 646–658.
18 M. Rumayor, J. Corredor, M. J. Rivero and I. Ortiz, *J. Cleaner Prod.*, 2022, **336**, 130430.
19 G. M. Haselmann and D. Eder, *ACS Catal.*, 2017, **7**, 4668–4675.
20 E. V. Spinacé, A. O. Neto, T. R. R. Vasconcelos and M. Linardi, *J. Power Sources*, 2004, **137**, 17–23.
21 E. V. Spinacé, A. O. Neto, E. G. Franco, M. Linardi and E. R. Gonzalez, *Quim. Nova*, 2004, **27**, 648–654.
22 B. Dong, T. Liu, C. Li and F. Zhang, *Chin. Chem. Lett.*, 2018, **29**, 671–680.
23 J. Shi, J. Chen, Z. Feng, T. Chen, Y. Lian, X. Wang and C. Li, *J. Phys. Chem. C*, 2007, **111**, 693–699.
24 R. S. Das and Y. K. Agrawal, *Vib. Spectrosc.*, 2011, **57**, 163–176.
25 N. Lagopati, E. P. Tsilibary, P. Falaras, P. Papazafiri, E. A. Pavlatou, E. Kotsopoulou and P. Kitsiou, *Int. J. Nanomed.*, 2014, **9**, 3219–3230.
26 Y. Lou, J. Xu, Y. Zhang, C. Pan, Y. Dong and Y. Zhu, *Mater. Today Nano*, 2020, **12**, 100093.
27 X. Wang, S. C. Huang, T. X. Huang, H. S. Su, J. H. Zhong, Z. C. Zeng, M. H. Li and B. Ren, *Chem. Soc. Rev.*, 2017, **46**, 4020–4041.
28 G. M. Haselmann and D. Eder, *ACS Catal.*, 2017, **7**, 4668–4675.

© 2025 The Author(s). Published by the Royal Society of Chemistry

Open Access Article. Published on 20 February 2025. Downloaded on 2/20/2026 6:57:31 AM.
This article is licensed under a Creative Commons Attribution-NonCommercial 3.0 Unported Licence.

29 E. Skliri, I. Vamvasakis, I. T. Papadas, S. A. Choulis and G. S. Armatas, *Catalysts*, 2021, **11**, 1–16.
30 E. Wolthuis, S. Kolk and L. Schaap, *Anal. Chem.*, 1954, **26**, 1238–1240.
31 A. Gopakumar, P. Ren, J. Chen, B. V. Manzolli Rodrigues, H. Y. Vincent Ching, A. Jaworski, S. Van Doorslaer, A. Rokicińska, P. Kuśtrowski, G. Barcaro, S. Monti, A. Slabon and S. Das, *J. Am. Chem. Soc.*, 2022, **144**, 2603–2613.
32 H. Li, B. Zhu, J. Sun, H. Gong, J. Yu and L. Zhang, *J. Colloid Interface Sci.*, 2024, **654**, 1010–1019.
33 G. Iervolino, D. Sannino, G. Pepe, M. Giovanna Basilicata, P. Campiglia and V. Vaiano, *Chem. Eng. J.*, 2023, **468**, 143725.
34 L. Yu, Y. Shao and D. Li, *Appl. Catal., B*, 2017, **204**, 216–223.
35 L. Yu and D. Li, *Catal. Sci. Technol.*, 2017, **9**, 635–640.

© 2025 The Author(s). Published by the Royal Society of Chemistry